The International Journal of Cardiovascular Imaging (2019) 35:771–779
https://doi.org/10.1007/s10554-018-1510-2

ORIGINAL PAPER

Anthracycline induced inconsistent left ventricular segmental systolic function variation in patients with lymphoma detected by three-dimensional speckle tracking imaging

Yuchen Xu[1,2] · Jing Shi[1,2] · Rui Zhao[1,2] · Chujie Zhang[1,2] · Yiyao He[1,2] · Jinyi Lin[3] · Qunling Zhang[4] · Xianhong Shu[1,2] · Leilei Cheng[1,2]

Received: 17 September 2018 / Accepted: 24 November 2018 / Published online: 25 January 2019

Abstract

Chemotherapy contained anthracycline inevitably cause declines of cardiac function. This study evaluated the deterioration of left ventricular segmental systolic function in patients with lymphoma received anthracycline chemotherapy detected by echocardiographic three dimensional speckle tracking imaging (3D-STI). Sixty patients with newly diagnosed diffuse large B-cell lymphoma who received R-CHOP chemotherapy were enrolled. Three dimensional left ventricular global longitudinal strain (3D-GLS), three dimensional left ventricular global circumferential strain (3D-GCS) and three dimensional left ventricular longitudinal strain of different left ventricular segments (3D-LS) were measured by 3D-STI at baseline, after the completion of two cycles and four cycles of the regimen respectively. Compared with baseline, 3D-GLS reduced significantly after four cycles of anthracycline therapy ($P < 0.001$), while 3D-GCS showed no significant variation during the whole procedure (all $P > 0.05$). For individual segment, LS of apical anterior and septal walls decreased significantly after two cycles of chemotherapy (all $P < 0.05$). After four cycles of treatment, 3D-LS of the mid-ventricular level (all $P < 0.05$), apical level (all $P < 0.05$) and apex ($P < 0.05$) worsened. Serum hs-cTnT levels increased after anthracycline exposure ($P < 0.05$) and Serum hs-cTnT levels were correlated with 3D-GLS at the end of four cycles ($r = 0.12$, $P = 0.03$). Mean values of involved segmental 3D-LS of two and four cycles were both correlated with serum hs-cTnT levels at the end of both two and four cycles ($r = 0.368$, $P = 0.041$; $r = 0.79$, $p < 0.001$). 3D-STI evaluation of the LV provides an understanding of the segmental impairment of LV wall and the possible process of LV impairment in lymphoma patients after anthracycline chemotherapy.

Keywords Anthracycline · Cardiotoxicity · Left ventricular function · Strain · Echocardiography

Introduction

Anthracycline-based chemotherapy is recommended as a standard treatment of a wide spectrum of hematologic malignancies and solid tumors [1–3], considering its definite antitumor effect. Unfortunately, the clinical use of these drugs is hampered because of the dose-dependent cardiotoxicity. Previous researches demonstrated that 57% of the patients receiving anthracycline would be subjected to impaired cardiac function. And 16–20% of them progressed to congestive heart failure ultimately which was associated with poor prognosis [4]. Therefore, it is imperative to detect anthracycline-induced cardiac injury in the early stage in order to, with the help of early pharmacologic intervention, preventing the occurrence of clinical heart failure. Recently, echocardiographic speckle tracking imaging has demonstrated promise as a tool of measuring subclinical cardiotoxicity

Yuchen Xu and Jing Shi have contributed equally to this work.

✉ Leilei Cheng
cheng.leilei@zs-hospital.sh.cn

1 Department of Echocardiography, Zhongshan Hospital, Fudan University, 180 Fenglin Road, Shanghai 200032, China

2 Shanghai Institute of Cardiovascular Diseases, Shanghai Institute of Medical Imaging, Fudan University, 180 Fenglin Road, Shanghai 200032, China

3 Department of Cardiology, Zhongshan Hospital, Shanghai Institute of Cardiovascular Diseases, Fudan University, 180 Fenglin Road, Shanghai, China

4 Department of Medical Oncology, Fudan University Shanghai Cancer Center, Shanghai, China

[5, 6]. With the combination of three-dimensional imaging and speckle tracking technique, three-dimensional speckle tracking imaging (3D-STI) is conducted in clinical application to analyze the spatial motions of myocardium. Previous 3D-STI studies mainly focused on global left ventricular function changes during chemotherapy. However, in fact, many middle-aged and elderly cancer patients with pre-existing coronary heart disease need to be handled with extreme caution before significant changes in integral function exists. Therefore, we designed this research to evaluate the changes of longitudinal strain of different left ventricular segments as well as the global longitudinal strain detected by 3D-STI in patients with lymphoma receiving anthracycline.

Methods

Subjects

Sixty patients with newly diagnosed diffuse large B cell non-Hodgkin lymphoma (DLBCL) between December 2012 and March 2016 at Fudan University Shanghai Cancer Center were studied retrospectively. The mean age of these patients was 52 years old, with a range of 20–78 years old. All patients were treated with R-CHOP contained anthracycline (cyclophosphamide: 750 mg/m^2, vincristine: 1.4 mg/m^2 up to a maximum dose of 2 mg/m^2, epirubicin which is a typical kind of anthracycline: 50–70 mg/m^2 on day 1, prednisone: 100 mg/m^2 on days 1–5 and rituximab: 375 mg/m^2). Cycles were administered every 21 days for a maximum of eight cycles. None of the patients received other cardiotoxicity agents, radiation therapy or cardiac protective protocols during the procedure. We excluded patients with: (1) history of valvular heart disease; (2) any known causes of cardiomyopathy; (3) serious arrhythmia; (4) history of congenital heart disease; (5) severe hypertension; (6) a previous history of heart failure and/or coronary artery disease, patients with indistinct ultrasound images were also excluded.

Echocardiography

All subjects underwent traditional two dimensional echocardiography, tissue Doppler imaging (TDI) as well as 3D-STI at baseline, at the end of two cycles and after the completion of four cycles. A commercially available system (iE33, Philips Medical Systems, Andover, WA, USA) equipped with S5-1 (1–5 MHz) and X3-1 (1–3 MHz) was used. Standard two dimensional and three dimensional echocardiography were performed according to the recommendations of American Society of Echocardiography [7]. Four consecutive cardiac cycles for two dimensional images and six consecutive cardiac cycles for 3D-STI images were acquired during a period of stable heart beat using the same system. Image parameters such as depth, sector size, angle and focus were adjusted to optimize the frame rate with a range of 60–80 FPS (frames per second) for two dimensional and 30–45 FPS for 3D-STI analysis. The technicians as well as the offline echo readers were blinded to the clinical data.

Echocardiographic examination

LV end-diastolic diameter (EDD), LV end-systolic diameter (ESD) were measured on the parasternal long-axis view by M-mode echocardiography. LV volumes and EF were assessed by means of the biplane Simpson's rule using manual tracing of digital images. The pulsed-wave Doppler-derived transmitral velocity and mitral annular velocity derived from digital color tissue Doppler imaging were obtained from apical four-chamber views. The E-wave deceleration time were measured by means of pulsed-wave Doppler recording. Mitral annular peak systolic myocardial velocity derived from color TDI was obtained from the septal mitral annulus.

Right ventricular end-diastolic area (RVEDA), right ventricular end- systolic area (RVESA) and right ventricular fractional area change (RVFAC) was obtained from the apical four-chamber view by tracing the RV endocardium both in systole and diastole from the annulus, along the free wall to the apex, and then back to the annulus along the interventricular septum.

$$\mathrm{RVFAC} = \frac{\text{RV end diastolic area} - \text{RV end systolic area}}{\text{RV end diastolic area}\,\%}$$

TAPSE was acquired by placing an M-mode cursor through the tricuspid annulus in the apical 4 chamber view and measuring the amount of longitudinal motion of the annulus at peak systole.

Three dimensional echocardiographic imaging was performed at the cardiac apex, using a X3-1 (1–3 MHz). Three dimensional full-volume data sets combining four sub-volumes were captured over four consecutive cardiac cycles. All three dimensional echocardiographic images were stored for offline analysis by TomTec software.

Analysis of 3D-STI

TomTec 4D LV analysis (4.6.0.411, TomTec Imaging Systems GMBH, Germany) was performed for 3D-STI data analysis based on the data set with the best image quality. LV data were interpreted with 4D LV-Function (TomTec Imaging Systems) software by making two reference points at the middle of mitral valve annulus and the apex respectively in three long-axis reference planes (apical four-chamber, two-chamber, and three-chamber views) and orientating one reference points at the annulus aortic valve in short-axis reference plane. The

endocardium and epicardium were retraced automatically to attain suitable tracking and small adjustments would be made to make the tracking more accurate. Three dimensional left ventricular global longitudinal strain (3D-GLS), three-dimensional left ventricular global circumferential strain (3D-GCS) and three-dimensional left ventricular longitudinal strain (3D-LS) on seventeen left ventricular segments (six basal, six mid, four apical and apex) were automatically calculated by the software based on the American Society of Echocardiography 17-segment model [8].

Serum biochemical markers assays

Serial serum samples were collected at baseline, after two cycles of the regimen and at four cycles of the regimen simultaneously. Blood was collected into EDTA tubes, centrifuged at 3500 × *g* for 20 min. The serum was drawn off and stored at − 80 °C. High-sensitivity cardiac troponin T (hs-cTnT) was measured using the hs-cTnT one-step electrochemiluminescence immunoassay (Roche cobase 411, Roche Diagnostics, Penzberg, Germany). Based on manufacturer's statement, in the analysis, undetectable hs-cTnT levels were considered to be < 0.002 ng/mL. Technologists recording the hs-cTnT were blind to the participants of clinical and echocardiography.

Inter-observer and intra-observer variability

Intra- and inter-observer reproducibility were assessed by calculating the difference between the values of 15 randomly selected patients measured by one observer twice and by a second observer.

Statistical analysis

Continuous data were expressed as mean ± standard deviation (SD). Differences at baseline, after two cycles of therapy and after four cycles of therapy were determined using one-way analysis of variance (ANOVA) for continuous data. Data were analyzed using standard statistical software (SPSS version 19.0; SPSS, Inc., Chicago, IL, USA). For all statistical evaluation of the results, values of $P < 0.05$ were considered significant. Inter- and intra-observer reproducibility of 3D-GLS, 3D-GCS and 3D-LS derived from 3D-STI were assessed using intraclass correlation coefficients from 10 randomly selected subjects.

Results

Baseline characteristics

After two and four cycles of chemotherapy, LVEDD (mm) and RVESA (cm^2) became larger than baseline (all $P < 0.05$). RVFAC (%) also increased after two and four cycles (all $P < 0.05$)

Other clinical characteristics and conventional echocardiographic parameters were similar at baseline, at the end of two cycles and four cycles of the chemotherapy (all $P > 0.05$) (Table 1).

3D-STI parameters

There was no significant difference between 3D-GLS at baseline and at the end of the first two cycles of anthracycline chemotherapy ($P = 0.154$), but 3D-GLS decreased after four cycles of exposure ($P < 0.001$). No significant changes of 3D-GCS were detected during the whole study ($P = 0.061$; $P = 0.058$) (Fig. 1).

After two cycles of chemotherapy, decrease of 3D-LS was observed in only two segments, which were apical anterior and septal wall (− 22.01 ± 7.99% vs. − 17.33 ± 6.82%, $P = 0.014$; − 24.27 ± 6.74% vs. − 17.91 ± 5.42%, $P = 0.002$). After four cycles of treatment, 3D-LS of all mid segments (anterior, anteroseptal, inferoseptal, inferior, inferolateral, anterolateral: − 17.85 ± 4.22% vs. − 14.72 ± 3.65%, $P < 0.001$; − 19.75 ± 4.47% vs. − 17.39 ± 4.02%, $P = 0.001$; -21.32 ± 4.09% vs. − 18.91 ± 3.91%, $P = 0.006$; − 21.49 ± 4.78% vs. − 19.29 ± 4.39%, $P = 0.024$; − 20.60 ± 5.84% vs. − 17.98 ± 5.13%, $P = 0.033$; − 18.90 ± 5.02% vs. − 15.72 ± 5.71%, $P = 0.004$, respectively), all apical segments (anterior, septal, inferior, lateral: -22.01 ± 7.99% vs. − 15.28 ± 5.26%, $P < 0.001$; − 24.27 ± 6.74% vs. − 17.91 ± 5.42%, $P < 0.001$; − 19.28 ± 3.63% vs. − 16.79 ± 2.73%, $P < 0.001$; − 20.98 ± 8.76% vs. − 17.07 ± 5.44%, $P = 0.026$, respectively) as well as apex (− 19.28 ± 3.63% vs. − 16.79 ± 2.73, $P < 0.001$) (Fig. 2) decreased markedly. Mean serum hs-cTnT levels of all patients increased significantly after two cycles as well as four cycles (0.003 ± 0.000 ng/mL vs. 0.013 ± 0.002 ng/mL vs. 0.022 ± 0.001 ng/mL, $P < 0.05$). Serum hs-cTnT levels were correlated with 3D-GLS of four cycles ($r = 0.12$, $P = 0.03$). Mean values of involved segmental 3D-LS were correlated with serum hs-cTnT levels at the end of two cycles and four cycles. ($r = 0.368$, $P = 0.041$; $r = 0.79$, $P < 0.001$) (Fig. 3). While, there was no correlation between 3D-GCS and hs-cTnT ($P > 0.05$).

Reproducibility

The intra-class correlation coefficients for intra-observer reproducibility of speckle tracking indices were 0.956 for 3D-GLS, 0.963 for 3D-GCS, 0.948 for 3D-LS, while the corresponding coefficients for inter-observer reproducibility were 0.936, 0.920 and 0.930, respectively.

Table 1 Clinical and conventional echocardiography characteristics

	Baseline	Two cycles	P-value	Four cycles	P-value
Age (years)	52 ± 14				
Gender (male/female)	35/25				
Mass (kg)	63 ± 14				
Heart rate (bpm)	80.6 ± 11.6	83.1 ± 12.7	0.330	82.6 ± 12.3	0.225
Cumulative doxorubicin dose (mg/kg)	0	118 ± 15.3		238 ± 21.8	
Left ventricular end-diastolic diameter (mm)	45.8 ± 3.5	45.7 ± 3.2	0.830	45.6 ± 3.6	0.810
Left ventricular end-systolic diameter (mm)	29.2 ± 3.2	28.9 ± 3.4	0.735	28.7 ± 3.0	0.702
End-diastolic thickness of the interventricular septum (mm)	8.6 ± 1.3	8.5 ± 1.4	0.808	8.5 ± 1.5	0.792
End-diastolic thickness of the posterior wall (mm)	8.4 ± 1.6	8.4 ± 1.5	0.989	8.3 ± 1.3	0.921
Left atrial diameter (mm)	34.1 ± 1.2	35.2 ± 2.1	0.865	36.4 ± 1.8	0.605
Left ventricular end-diastolic volume (ml)	63.9 ± 16.7	66.5 ± 19.0	0.305	66.9 ± 16.6	0.198
left ventricular end-systolic volume (ml)	26.6 ± 9.5	29.8 ± 8.6	0.011*	30.5 ± 10.3	0.024*
left ventricular ejection fraction (%)	57.7 ± 8.5	55.6 ± 8.2	0.193	55.3 ± 6.1	0.052
Mitral annular peak systolic velocity (cm)	11.3 ± 2.3	11.5 ± 3.1	0.072	11.0 ± 2.7	0.069
Deceleration time of mitral inflow E velocity	176. 3 ± 32.1	182.4 ± 33.5	0.382	186.5 ± 34.8	0.356
Right ventricular end-diastolic area (cm^2)	15.1 ± 3.8	14.7 ± 3.4	0.181	14.4	0.067
Right ventricular end- systolic area (cm^2)	9.0 ± 2.3	8.1 ± 2.1	0.000*	8.1 ± 1.9	0.000*
Right ventricular fractional area change (%)	40.2 ± 5.9	44.6 ± 4.2	0.000*	43.4 ± 4.9	0.001*
Tricuspid annular plane systolic excusion (mm)	21.6 ± 0.3	21.4 ± 0.2	0.570	21.3 ± 0.2	0.352

Data are presented as mean ± SD

*Compared with baseline, left ventricular end-systolic volume showed significant variation after two cycles of chemotherapy ($P < 0.05$)

Discussion

Our study used 3D-STI to evaluate the variation of left ventricular global and segmental systolic function in patients with lymphoma received anthracycline chemotherapy. Main findings of this study are (1) 3D-GLS reduced significantly after four cycles of anthracycline therapy, while no significant changes of 3D-GCS were detected during the whole study. (2) LS of apical anterior and septal wall decreased after two cycles, and 3D-LS of all mid-ventricular levels, apical levels and apex dropped after four cycles. (3) Serum hs-cTnT levels increased significantly after two and four cycles, and serum hs-cTnT levels were correlated with 3D-GLS as well as 3D-LS. This research may be the earliest report about the segmentally different changes of 3D-LS of left ventricle in patients with lymphoma received anthracycline treatment.

Anthracycline is widely used as anti-cancer chemotherapeutic agents. However, its application is limited due to the irreversible cardiotoxicity. Chemotherapy-related cardiac dysfunction (CTRCD) is one of the anthracycline-induced cardiotoxicity, occurring in 9% of patients, and 98% of the cases occurred within the first year [9]. Considering the serious consequences of cardiotoxicity, early detection of subclinical myocardial dysfunction as well as prompt initiation of heart failure treatment should be applied to improve the patients' survival rate. Echocardiography has been recommended as the method of choice for the detection of myocardial dysfunction before, during and after cancer therapy [10]. 2D Simpson's LVEF is widely used in clinic as the traditional echocardiographic parameter assessing left ventricular systolic function. However, decreased LVEF has been proved to be a late phenomenon of chemotherapy-related cardiotoxicity. Studies showed that although therapeutic interventions was taken once the LVEF decreased markedly (decline in initial LVEF of at least 5% and < 55%), more than 58% of patients still failed to recover systolic function [11, 12]. Moreover, changes of LVEF might not be consistent with cardiac biopsy grades. Myocardium could be severe affected even though LVEF was still within normal range [13] (Fig. 4).

Low sensibility of LVEF in monitoring early stage of cardiac systolic disfunction after anthracycline therapy and the rapidly emerging ultrasound technologies have resulted in a series of studies focusing on the application of new ultrasonic tools in early detection of cardiotoxicity. Three-dimensional (3D) echocardiographic (3DE) imaging represents a major innovation in cardiovascular ultrasound imaging. It can provide real-time 3D images of cardiac structures from any spatial point of view and evaluate cardiac chamber volumes and mass, which avoids geometric assumptions. The value of 3DE in assessment of regional left ventricular wall motion and quantification of systolic dyssynchrony has been demonstrated [14].The speckle tracking image is an

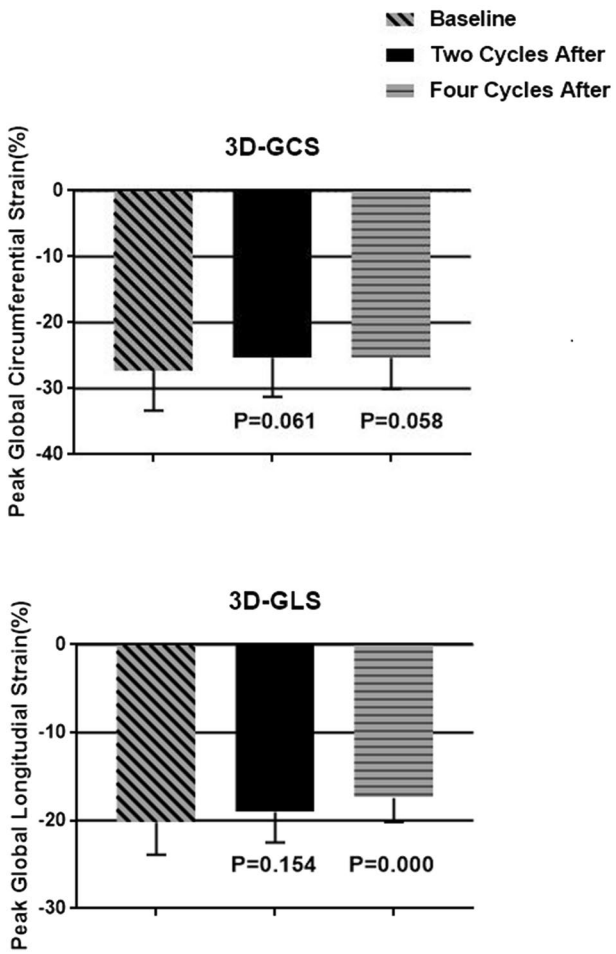

Fig. 1 Bar graphs of 3D-GCS and 3D-3D-GLS. 3D-GLS after four cycles showed significant difference compared with baseline (P = 0.000), 3D-GCS showed no significant variation during the whole procedure

image-processing algorithm which can analyze motion by tracking natural acoustic reflections and interference patterns within an ultrasonic window, which resolves angle-independent of tissue Doppler Imaging [15]. As the combination of 3DE and STI, three dimensional speckle tracking imaging (3D-STI) can be used to analyze the spatial motion of myocardium in three-dimensional level and can provide novel deformation parameters (3D-strain, rotation, twist, etc.) that have the potential to carry out more accurate evaluation of global and regional cardiac function. The reliability and feasibility of 3D-STI have been validated and the utility of 3D-STI have been increasingly explored in cardiovascular imaging centres [16]. In the past five years, researches on using 3D-STI to evaluate impairment of cardiac function caused by chemotherapy has never been stopped. Among several novel parameters of 3D-STI, although controversial, global longitudinal strain (GLS) remains to be the best measure in early detection of cardiotoxicity [17, 18] and has been accepted in position papers and expert recommendations [10, 19]. Our previous research analyzed 3D global strain of LV in patient received anthracycline and got the same conclusion [20]. The number of cancer survivors is increasing and the survival period of them is prolonged [21]. Some of them are patients with cardiovascular disease who develop cancer, while others can develop new myocardial ischemia like coronary heart disease as they grow older. Moreover, chemotherapy as well as radiotherapy are both risk factors for coronary heart disease [22, 23]. Therefore, for chemotherapy, it is far from enough to evaluate the overall left ventricular function only. Segmental myocardial situation should be monitored regularly in cancer patients. Kapusta's research showed that anthracycline therapy might cause left ventricular regional wall motion abnormalities and mechanical dyssynchrony [24]. However, their research was based on 2D-tissue doppler imaging and the motion abnormalities were only described in LV free wall. Therefore, we hypothesized that the impairment of different ventricular segments resulted from anthracycline could be detected by 3D-STI. In order to explore the possible sequence of anthracycline-induced segmental impairment, we made a detailed segmental function analysis of different left ventricular segments and found that 3D-LS of apical anterior and septal walls decreased significantly after two cycles of chemotherapy, and 3D-LS of apical and middle segment dropped after four cycles of chemotherapy, while 3D-LS of basal segments remained stable (Fig. 5). These findings suggest that anterior and septal walls of the LV are more sensitive to drug toxicity than basal wall and the development of cardiotoxicity may start from apical segment to basal.

One possible interpretation of this heterogeneity may be related with the blood supply of myocardium. Anterior and septal walls are fed by middle-distal coronary. Compared with proximal coronary, middle-distal coronary has smaller vessel diameter and its blood supply can be affected by proximal vessel [25, 26]. The blood supply of anterior and septal segments is notably more insufficient than the basal part. Moreover, the blood flow will exert pressure on vessel wall, including the wall shear stress (WSS) which is parallel to the flow direction and the compressive stress which is perpendicular to the flow direction [27]. Studies have shown that WSS would generally decrease as the coronary extend from proximal to distal part [28, 29]. Low WSS would trigger local inflammatory responses and vascular injury culminating in endothelial dysfunction and make endothelial cells higher susceptibility to toxic chemicals [30]. Hence, apical and middle segments are particularly vulnerable to anthracycline-induced cardiotoxicity.

In addition, this segmental difference may also be related to myocardial mechanics of the left ventricle. Previous study had analysed time-twist sequence of left ventricular (twist is referred to the rotation of a short-axis

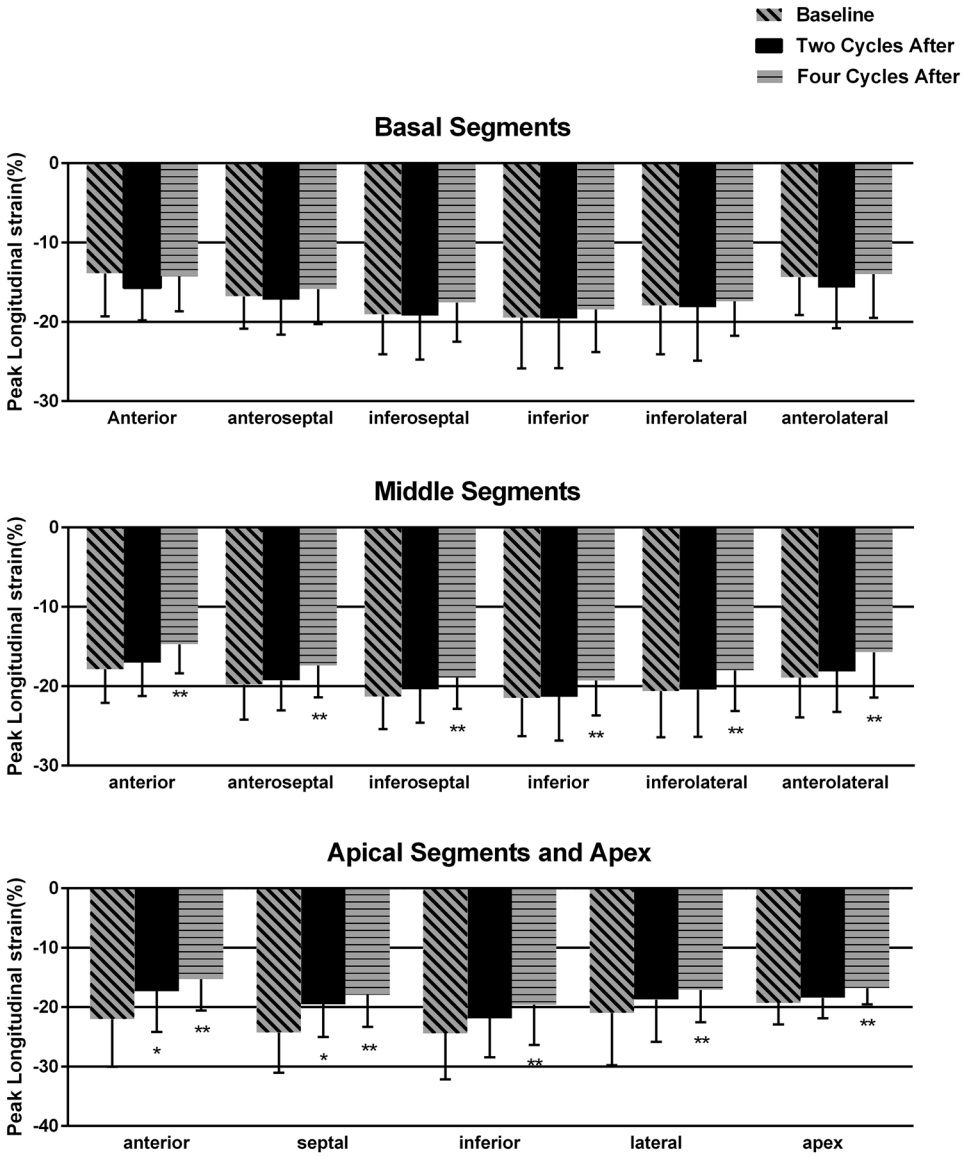

Fig. 2 Bar graphs of segmental 3D-LS of the left ventricle. *Compared with baseline, LS on apical anterior and apical septal walls showed significant variation after two cycles of chemotherapy ($P < 0.05$). **All LS on middle and apical segments showed significant decrease after four cycles anthracycline chemotherapy ($P < 0.05$)

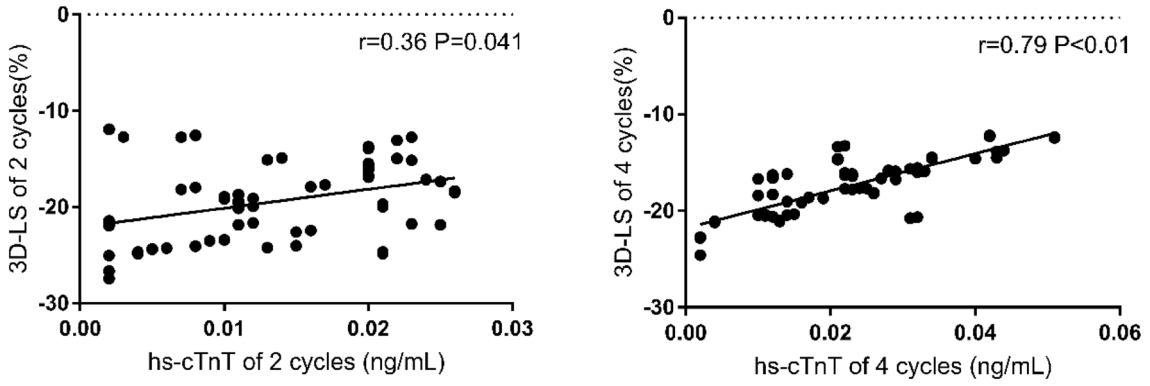

Fig. 3 Dot plot showing the relationship between 3D-LS and hs-cTnT of two cycles (left) and four cycles (right). 3D-LS of two and cycles are calculated as mean value of 3D-LS of apical and middle wall

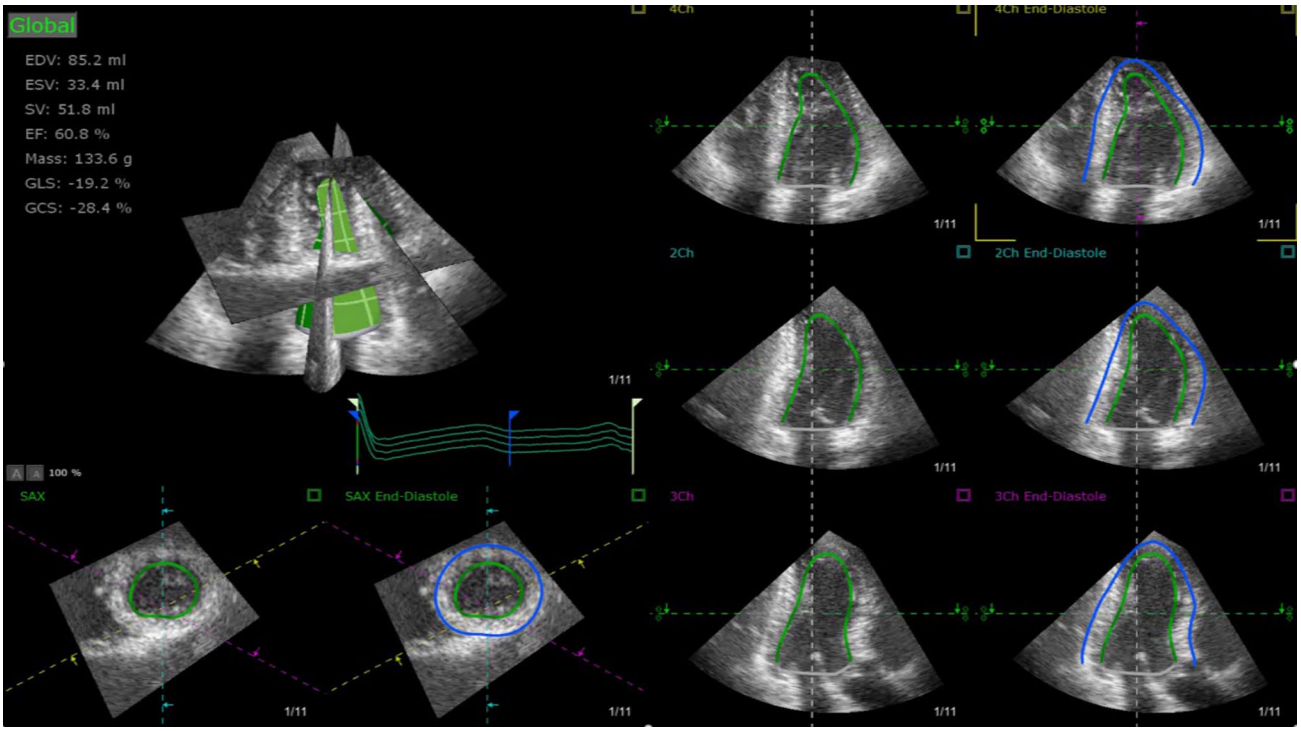

Fig. 4 Example of left ventricule three-dimensional strain analysis using TomTec offline analysis software (4.6.0.411, TomTec Imaging Systems GMBH, Germany). Tracing of left ventricular end-diastolic and end-systolic endocardial borders in the apical four-chamber, two-chamber, and three-chamber view as well as short-axis view respectively

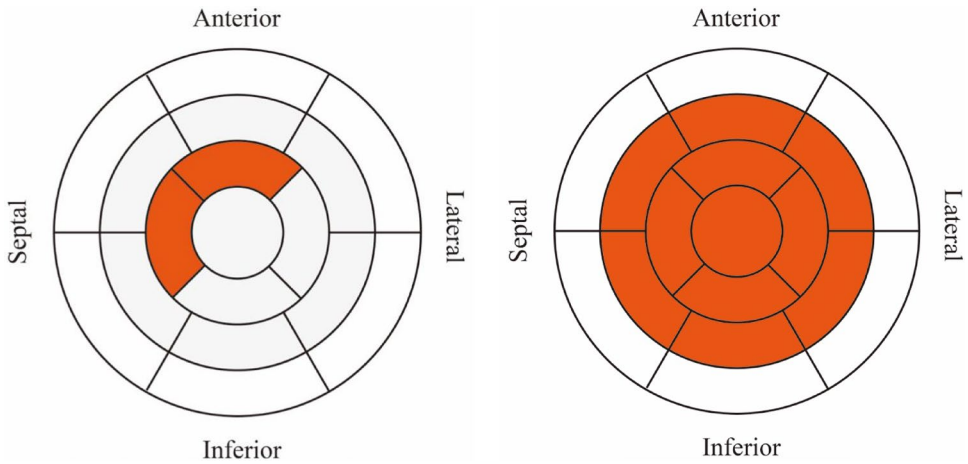

Fig. 5 Seventeen segment bull's eye maps of left ventricule after two cycles (left) and four cycles (right) of chemotherapy. The segments' 3D-LS which decreased significantly ($P < 0.05$) has been highlighted in orange

sections of left ventricle) and found that rotation of the basal segment is significantly lower than apical segment in magnitude [31]. Moreover, compared to the base, myocardium shortening in the apical and middle wall is higher, observed as a strain gradient in the base-apex axis [32]. Based on this we presumed that the myocardium of apical and middle wall does more work and requires more oxygen than basal part, which can be another interpretation of the susceptibility of apical and middle wall. Therefore, a long-term follow-up of lymphoma patients should be done to explore the change of the basal wall. This finding may help physician to adjust the antitumor regimens and may suggest a need for early cardiac protections individually.

Increase of serum hs-cTnT levels is the gold diagnostic standard of myocardial injury [33]. The hs-cTnT levels increased after two and four cycles of chemotherapy which further testified the decrease of 3D-LS of left ventricular segments.

Limitations of the study

Several limitations to this study warrant comments. First, our study investigated a small number and short follow-up of patients in single-center. Further studies is needed to verify our findings. Second, accuracy of 3D-STI analysis depends on the definition of the image. To ensure the image quality, we told patients to hold the breath and kept still, adjusting an appropriate gain, changing the probe position to make the structure of interest be perpendicular to the ultrasound beam. Despite this, quality of a part of images is still imperfect and the accuracy of analysis would be affected slightly. Third, patients in this study also be treated with other chemotherapy drugs such as cyclophosphamide, which may also cause cardiotoxicity that is indistinguishable from anthracyclines. However, according to the literature, anthracycline is more cardiotoxic than these chemotherapy drugs.

Conclusion

Despite preserved left ventricular ejection fraction, subclinical LV systolic dysfunction was present in anthracycline-chemotherapy patients. Segmental longitudinal strain decreased at the early phase of myocardial injury and the preferential impairment occurred in the apex. 3D-STI evaluation of the LV provides an understanding of the segmental impairment of the LV wall and the possible process of LV impairment in lymphoma patients after anthracycline chemotherapy.

Funding This study was supported by grant 2017BR027 from Municipal Human Resources Development Program for Outstanding Leaders in Medical Disciplines in Shanghai, grant 20164Y0076 from Shanghai Health and Family Planning Commission, 81771840 from National Natural Science Foundation of China.

Compliance with Ethical Standards

Conflict of interest All authors declare no conflicts of interest.

Ethical approval All procedures performed in studies involving human participants were in accordance with the ethical standards of the institutional and/or national research committee and with the 1964 Helsinki declaration and its later amendments or comparable ethical standards.

Informed consent Informed consent was obtained from all individual participants included in the study.

References

1. National Comprehensive Cancer Network (2015) Clinical practice guidelines in oncology. Breast Cancer, Version1. IOP Publishing PhysicsWeb. https://www.nccn.org/professionals/physician_3D-GLS/f_guidelines.asp,2015
2. National Comprehensive Cancer Network (2015) Clinical practice guidelines in oncology. Gastric Cancer, Version1. IOP Publishing PhysicsWeb https://www.nccn.org/professionals/physician_3D-GLS/f_guidelines.asp,2015
3. National Comprehensive Cancer Network (2015) Clinical practice guidelines in oncology. Hodgkin's lymphoma, Version1. IOP Publishing PhysicsWeb https://www.nccn.org/professionals/physician_3D-GLS/f_guidelines.asp,2015
4. Van der pal HJ, Van dalen EC, Van delden E et al (2012) High risk of symptomatic cardiac events in childhood cancer survivors. J Clin Oncol 30:1429–1437
5. Okuma H, Noto N, Tanikawa S, Kanezawa K, Hirai M, Shimozawa K, Yagasaki H, Shichino H, Takahashi S (2017) Impact of persistent left ventricular regional wall motion abnormalities in childhood cancer survivors after anthracycline therapy: assessment of global left ventricular myocardial performance by 3D speckle-tracking echocardiography. J Cardiol 70:396–401
6. Çetin S, Babaoğlu K, Başar EZ, Deveci M, Çorapçıoğlu F (2018) Subclinical anthracycline-induced cardiotoxicity in long-term follow-up of asymptomatic childhood cancer survivors: assessment by speckle tracking echocardiography. Echocardiography 35:234–240
7. Lang RM, Bierig M, Devereux RB, Flachskampf FA, Foster E, Pellikka PA, Picard MH, Roman MJ, Seward J, Shanewise JS, Solomon SD, Spencer KT, Sutton MS, Stewart WJ (2005) Recommendations for chamber quantification: a report from the american society of echocardiography's guidelines and standards committee and the chamber quantification writing group, developed in conjunction with the european association of echocardiography, a branch of the European Society of Cardiology. J Am Soc Echocardiogr 18:1440–1463
8. Cerqueira MD, Weissman NJ, Dilsizian V, Jacobs AK, Kaul S, Laskey WK, Pennell DJ, Rumberger JA, Ryan T, Verani MS (2002) Standardized myocardial segmentation and nomenclature for tomographic imaging of the heart. A statement for healthcare professionals from the Cardiac Imaging Committee of the Council on Clinical Cardiology of the American Heart Association. Int J Cardiovasc Imaging 18:539–542
9. Cardinale D, Colombo A, Bacchiani G, Tedeschi I, Meroni CA, Veglia F, Civelli M, Lamantia G, Colombo N, Curigliano G, Fiorentini C, Cipolla CM (2015) Early detection of anthracycline cardiotoxicity and improvement with heart failure therapy. Circulation 131:1981–1988
10. Zamorano JL, Lancellotti P, Rodriguez Muñoz D, Aboyans V, Asteggiano R, Galderisi M, Habib G, Lenihan DJ, Lip G, Lyon AR, Lopez Fernandez T, Mohty D, Piepoli MF, Tamargo J, Torbicki A, Suter TM (2016) 2016 ESC position paper on cancer treatments and cardiovascular toxicity developed under the auspices of the ESC committee for practice guidelines: the task force for cancer treatments and cardiovascular toxicity of the European Society of Cardiology (ESC). Eur Heart J 37:2768–2801
11. Cardinale D, Colombo A, Lamantia G, Colombo N, Civelli M, De Giacomi G, Rubino M, Veglia F, Fiorentini C, Cipolla CM (2010) Anthracycline-induced cardiomyopathy: clinical relevance and response to pharmacologic therapy. J Am Coll Cardiol 55:213–220
12. Cardinale D, Colombo A, Torrisi R, Sandri MT, Civelli M, Salvatici M, Lamantia G, Colombo N, Cortinovis S, Dessanai MA, Nolè F, Veglia F, Cipolla CM (2010) Trastuzumab-induced cardiotoxicity: clinical and prognostic implications of troponin I evaluation. J Clin Oncol 28:3910–3916
13. Ewer MS, Ali MK, Mackay B, Wallace S, Valdivieso M, Legha SS, Benjamin RS, Haynie TP (1984) A comparison of cardiac

biopsy grades and ejection fraction estimations in patients receiving adriamycin. J Clin Oncol 2:112–117
14. Lang RM, Badano LP, Tsang W, Adams DH, Agricola E, Buck T, Faletra FF, Franke A, Hung J, de Isla LP, Kamp O, Kasprzak JD, Lancellotti P, Marwick TH, McCulloch ML, Monaghan MJ, Nihoyannopoulos P, Pandian NG, Pellikka PA, Pepi M, Roberson DA, Shernan SK, Shirali GS, Sugeng L, Ten Cate FJ, Vannan MA, Zamorano JL, Zoghbi WA (2012) EAE/ASE recommendations for image acquisition and display using three-dimensional echocardiography. J Am Soc Echocardiogr 25:3–46
15. Cameli M, Mondillo S, Galderisi M, Mandoli GE, Ballo P, Nistri S, Capo V, D'Ascenzi F, D'Andrea A, Esposito R, Gallina S, Montisci R, Novo G, Rossi A, Mele D, Agricola E (2017) Speckle tracking echocardiography: a practical guide. G Ital Cardiol (Rome) 18:253–269
16. Thavendiranathan P, Poulin F, Lim KD, Plana JC, Woo A, Marwick TH (2014) Use of myocardial strain imaging by echocardiography for the early detection of cardiotoxicity in patients during and after cancer chemotherapy: a systematic review. J Am Coll Cardiol 63:2751–2768
17. Santoro C, Arpino G, Esposito R, Lembo M, Paciolla I, Cardalesi C, de Simone G, Trimarco B, De Placido S, Galderisi M (2017) 2D and 3D strain for detection of subclinical anthracycline cardiotoxicity in breast cancer patients: a balance with feasibility. Eur Heart J Cardiovasc Imaging 18:930–936
18. Toro-Salazar OH, Ferranti J, Lorenzoni R, Walling S, Mazur W, Raman SV, Davey BT, Gillan E, O'Loughlin M, Klas B, Hor KN (2016) Feasibility of echocardiographic techniques to detect subclinical cancer therapeutics-related cardiac dysfunction among high-dose patients when compared with cardiac magnetic resonance imaging. J Am Soc Echocardiogr 29:119–131
19. Curigliano G, Cardinale D, Suter T, Plataniotis G, de Azambuja E, Sandri MT, Criscitiello C, Goldhirsch A, Cipolla C, Roila F (2012) Cardiovascular toxicity induced by chemotherapy, targeted agents and radiotherapy: ESMO clinical practice guidelines. Ann Oncol 23(Suppl 7):i155–i166
20. Song FY, Shi J, Guo Y, Zhang CJ, Xu YC, Zhang QL, Shu XH, Cheng LL (2017) Assessment of biventricular systolic strain derived from the two-dimensional and three-dimensional speckle tracking echocardiography in lymphoma patients after anthracycline therapy. Int J Cardiovasc Imaging 33:857–868
21. Mariotto AB, Yabroff KR, Shao Y, Feuer EJ, Brown ML (2011) Projections of the cost of cancer care in the United States: 2010–2020. J Natl Cancer Inst 103:117–128
22. Van Nimwegen FA, Schaapveld M, Janus CP, Krol AD, Petersen EJ, Raemaekers JM, Kok WE, Aleman BM, van Leeuwen FE (2015) Cardiovascular disease after Hodgkin lymphoma treatment: 40-year disease risk. JAMA Intern Med 175:1007–1017
23. Cuomo JR, Javaheri SP, Sharma GK, Kapoor D, Berman AE, Weintraub NL (2018) How to prevent and manage radiation-induced coronary artery disease. Heart 104:1647–1653
24. Kapusta L, Groot-Loonen J, Thijssen JM, DeGraaf R, Daniëls O (2003) Regional cardiac wall motion abnormalities during and shortly after anthracyclines therapy. Med Pediatr Oncol 41:426–435
25. Zhang LR, Xu DS, Liu XC (2011) Coronary artery lumen diameter and bifurcation angle derived from CT coronary angiographic image in healthy people. Zhonghua xin xue guan bing za zhi 39(12): 1117–1123
26. Medrano-Gracia P, Ormiston J, Webster M, Beier S, Young A, Ellis C, Wang C, Smedby Ö, Cowan B (2016) A computational atlas of normal coronary artery anatomy. EuroIntervention 12(7): 845–854
27. Cecchi E, Giglioli C, Valente S, Lazzeri C, Gensini GF, Abbate R, Mannini L (2011) Role of hemodynamic shear stress in cardiovascular disease. Atherosclerosis 214:249–256
28. Salvucci FP, Perazzo CA, Gurfinkel E, Armentano RL, Barra JG (2010) A patient-specific method for the evaluation of wall shear stress in human coronary arteries. Conf Proc IEEE Eng Med Biol Soc 2010:3788–3791
29. Pinto SI, Campos JB (2016) Numerical study of wall shear stress-based descriptors in the human left coronary artery. Comput Methods Biomech Biomed Eng 19:1443–1455
30. Siasos G, Sara JD, Zaromytidou M, Park KH, Coskun AU, Lerman LO, Oikonomou E, Maynard CC, Fotiadis D, Stefanou K, Papafaklis M, Michalis L, Feldman C, Lerman A, Stone PH (2018) Local low shear stress and endothelial dysfunction in patients with nonobstructive coronary atherosclerosis. J Am Coll Cardiol 71:2092–2102
31. Sengupta PP, Tajik AJ, Chandrasekaran K, Khandheria BK (2008) Twist mechanics of the left ventricle: principles and application. JACC Cardiovasc Imaging 1:366–376
32. Sengupta PP, Khandheria BK, Korinek J, Wang J, Jahangir A, Seward JB, Belohlavek M (2006) Apex-to-base dispersion in regional timing of left ventricular shortening and lengthening. J Am Coll Cardiol 47:163–172
33. Rubini Gimenez M, Badertscher P, Twerenbold R, Boeddinghaus J, Nestelberger T, Wussler D, Miró Ò, Martín-Sánchez FJ, Reichlin T, Mueller C (2018) Impact of the US food and drug administration-approved sex-specific cutoff values for high-sensitivity cardiac troponin t to diagnose myocardial infarction. Circulation 137:1867–1869